Disulfide Structure of the Leucine-Rich Repeat C-Terminal Cap and C-Terminal Stalk Region of Nogo-66 Receptor

Dingyi Wen,* Craig P. Wildes, Laura Silvian, Lee Walus, Sha Mi, Daniel H. S. Lee, Werner Meier, and R. Blake Pepinsky

Biogenidec, Inc., 14 Cambridge Center, Cambridge, Massachusetts 02142

Received August 30, 2005; Revised Manuscript Received October 14, 2005

ABSTRACT: Nogo-66 receptor (NgR1) is a leucine-rich repeat (LRR) protein that forms part of a signaling complex modulating axon regeneration. Previous studies have shown that the entire LRR region of NgR1, including the C-terminal cap of the LRR, LRRCT, is needed for ligand binding, and that the adjacent C-terminal region (CT stalk) of the NgR1 contributes to interaction with its coreceptors. To provide structure-based information for these interactions, we analyzed the disulfide structure of full-length NgR1. Our analysis revealed a novel disulfide structure in the C-terminal region of the NgR1, wherein the two Cys residues, Cys-335 and Cys-336, in the CT stalk are disulfide-linked to Cys-266 and Cys-309 in the LRRCT region: Cys-266 is linked to Cys-335, and Cys-309 to Cys-336. The other two Cys residues, Cys-264 and Cys-287, in the LRRCT region are disulfide-linked to each other. The analysis also showed that Cys-419 and Cys-429, in the CT stalk region, are linked to each other by a disulfide bond. Although published crystal structures of a recombinant fragment of NgR1 had revealed a disulfide linkage between Cys-266 and Cys-309 in the LRRCT region and we verified its presence in the corresponding fragment, this is artificially caused by the truncation of the protein, since this linkage was not detected in intact NgR1 or a slightly larger fragment containing Cys-335 and Cys-336. A structural model of the LRRCT with extended residues 311−344 from the CT stalk region is proposed, and its function in coreceptor binding is discussed.

Axonal regeneration in the central nervous system (CNS)[1] is inhibited by at least three myelin-associated proteins: myelin-associated glycoprotein (MAG), oligodendrocyte myelin glycoprotein (OMgp), and Nogo A (*1*−*6*). The inhibitory event is mediated in part by NgR1, which serves as a receptor for Nogo-66, MAG, and OMgp (*7*−*9*). NgR1 (Nogo-66 receptor) is a glycosylphosphatidylinositol (GPI) protein that forms a signaling complex with LINGO-1 and p75 or TAJ (also known as TROY), transducing the inhibitory signals intracellularly to the Rho family GTPases (*10*, *11*). NgR1 is a leucine-rich repeat (LRR) protein that contains eight LRRs flanked by N-terminal and C-terminal cysteine-rich domains (LRRNT and LRRCT regions, respectively) (residues 27−310) and a 135-residue Ser-, Thr-, Pro-, and Gly-rich stalk region (CT stalk) between the LRRCT region and the GPI anchor site. NgR1(310) (residues 27−310) is required and is sufficient for myelin ligand binding, while residues from the CT stalk region provide additional contacts with coreceptors, such as p75, TAJ, and LINGO-1 (*10*−*13*). Within NgR1(310) there are 10 cysteines, four in each of the LRRNT and LRRCT regions and two in the LRR region. The crystal structure of NgR1(310) shows that the disulfide linkages in the LRRNT and LRRCT regions are in the same order; i.e., the first Cys in the region is disulfide-linked to the third Cys in the module, and the second Cys is linked to the fourth Cys. On the basis of the crystal structure of NgR1(310), it has been suggested (*14*, *15*) that the evolutionarily conserved aromatic residue patches in the concave surface are probably degenerate ligand binding sites, and that the deep cleft at the C-terminal base of the LRR may play a role in association of NgR1 with the p75 coreceptor. The CT stalk region of NgR1 contains four Cys residues, Cys-335, Cys-336, Cys-419, and Cys-429; however, there is no structural information available for the CT stalk region of NgR1. To better understand the structure−function relationship of NgR1, we have analyzed the disulfide linkages in full-length NgR1 by enzymatic fragmentation, peptide mapping, and mass spectrometric analysis, focusing mainly on the CT stalk region. Surprisingly, our analysis revealed a novel disulfide structure in the LRRCT and C-terminal regions of the NgR1, and showed that the published disulfide structure for the LRRCT region of NgR1(310) is not representative of that found in full-length NgR1 and is likely

* To whom correspondence should be addressed. Telephone: (617) 679-2362. Fax: (617) 679-3635. E-mail: dingyi.wen@biogenidec.com.

[1] Abbreviations: NgR1, Nogo-66 receptor; LRR, leucine-rich repeat; LRRNT, LRR N-terminal cap; LRRCT, LRR C-terminal cap; CT stalk, C-terminal region of the NgR1; CNS, central nervous system; MAG, myelin-associated glycoprotein; OMgp, oligodendrocyte myelin glycoprotein; GPI, glycosylphosphatidylinositol; LINGO-1, LRR and Ig domain-containing Nogo receptor-interacting protein; TMAE, trimethylaminoethyl; Ni−NTA, nickel−nitrilotriacetic acid; GuHCl, guanidine hydrochloride; AP, alkaline phosphatase; FL, full-length; endo-Lys-C, endoprotease Lys-C; endo-Asp-N, endoprotease Asp-N; endo-Glu-C, endoprotease Glu-C; TCEP, tris(2-carboxyethyl)phosphine hydrochloride; NEM, *N*-ethylmaleimide; TFA, trifluoroacetic acid; DDA, data-dependent acquisition function; SEC, size exclusion chromatography; NES, *N*-ethylsuccinimidyl; TIC, total ion chromatogram; vWF-A1, von Willebrand factor A1 domain; MALDI-TOF MS, matrix-assisted laser desorption ionization time-of-flight mass spectrometry; ESI, electrospray ionization; CID, collision-induced dissociation.

10.1021/bi0517483 CCC: $30.25
Published on Web 11/24/2005

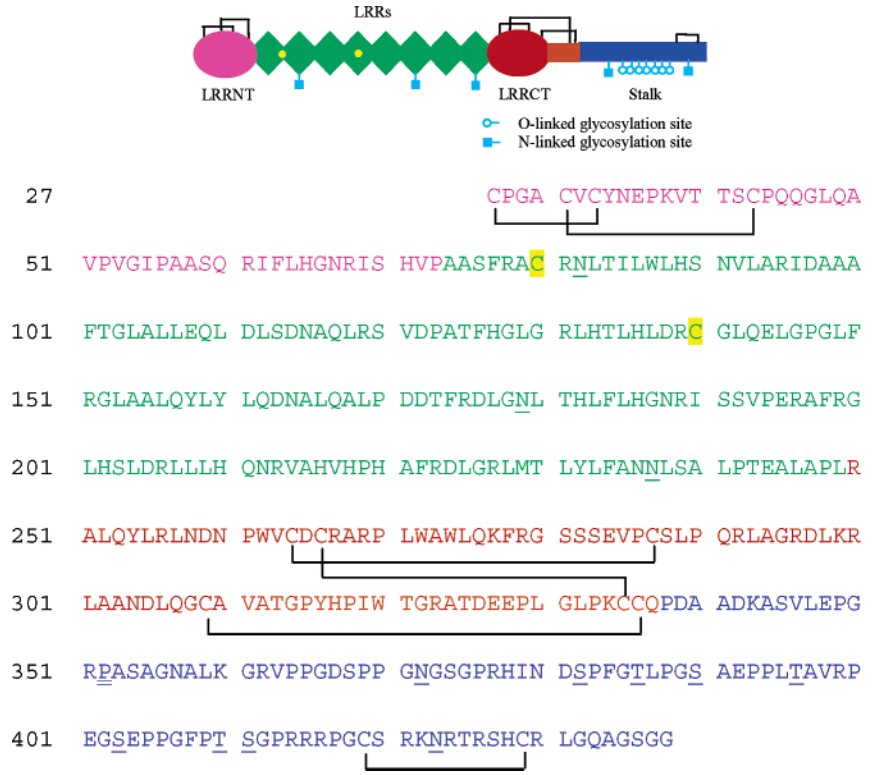

FIGURE 1: Schematic summary of key structural elements in the human FL-NgR1 sequence: LRRNT, magenta; eight LRR motifs, green; predicted LRRCT, red; extended LRRCT, orange; and stalk region, blue. Black lines represent disulfide bonds determined in this study. Cys residues in the free thiol form are highlighted in yellow. Hydroxyproline is double-underlined; glycosylation sites are underlined. Signal peptide and FLAG tag sequences are not shown.

caused by truncation of the protein. A structural model of the LRRCT with extended residues 311−344 from the CT stalk region has been proposed and reveals a possible area for protein−protein interaction. These structural findings with NgR1 reveal that the LRRCT region is larger than predicted, and as such has potential ramifications for deducing the structures of other LRR proteins that have been determined using minimal truncated domains from the LRR region.

MATERIALS AND METHODS

Protein Expression and Purification of NgR1 Proteins. Human full-length NgR1 (FL-NgR1, residues 27−438, Figure 1) with a flag tag at its N-terminus was expressed in CHO cells and purified as a soluble protein from the conditioned medium by sequential chromatography on TMAE-Fractogel (EM Merck) and Ni−NTA (Qiagen) agarose. Human NgR1(310) (residues 27−310) and human NgR1(344) (residues 27−344) were expressed as histidine-tagged proteins (C-terminal tag) in insect cells and purified by sequential chromatography on SP-Sepharose (Amersham BioSciences) and Ni−NTA agarose. Rat NgR1(344) (residues 27−344)−rat Fc(IgG1) fusion protein and rat NgR1-(310) (residues 27−310) were expressed in CHO cells. Rat NgR1(344)−rat Fc(IgG1) fusion protein was purified on protein A−Sepharose (Amersham Biosciences) and rat NgR1(310) on SP-Sepharose. Samples were analyzed for purity by SDS−PAGE on 4 to 20% gradient gels (NOVEX), and for aggregation by size exclusion chromatography (SEC) on a Superdex 200 column (Amersham Biosciences). The column was run in PBS at a flow rate of 20 mL/h and the column effluent monitored for absorbance at 280 nm.

Deglycosylation of NgR Proteins. N-Linked glycans were removed from the native proteins with PNGase F. Approximately 1 μL of PNGase F (2.5 milliunits/μL, Prozyme) was added to 25 μL of a solution containing ~20 μg of protein. The solution was incubated at 37 °C for 24 h; then an additional 1 μL of PNGase F was added, and the solution was kept at room temperature for an additional 24 h.

Alkylation of NgR1 Proteins. Alkylation was carried out under denaturing but nonreducing conditions. Approximately 0.3 μL of 4-vinylpyridine was added to 50 μL of the solution containing ~20 μg of protein, and immediately afterward 50 mg of guanidine hydrochloride (GuHCl) was added to the solution. The solution was incubated at room temperature in the dark for 60 min. The alkylated proteins were recovered by precipitation with 40 volumes of −20 °C ethanol (*16*). The solution was stored at −20 °C for 1 h and then centrifuged at 14000*g* for 8 min at 4 °C. The supernatant was discarded, and the precipitate (~20 μg/vial) was washed once with −20 °C ethanol.

Tryptic and Endoprotease Lys-C Digestion and Separation of Digested NgR1 Peptides. Approximately 20 μg each of the alkylated proteins, deglycosylated or fully glycosylated, was digested with 5% (w/w) endoprotease Lys-C (endo-Lys-C, Wako) in 1 M urea, 0.2 M Tris-HCl (pH 6.5), and 1 mM $CaCl_2$ for 5 h at room temperature; then 5% (w/w) trypsin (Promega) was added, and the solution was incubated for an additional 10−12 h at room temperature. The final volume was 55 μL. Prior to analysis of the digests on a LC−MS system, 55 μL of freshly prepared 8 M urea was added to improve peptide solubility, and then the solution was split into two parts: one was analyzed after reduction for 1 h at

37 °C with 40 mM DTT, and the other part was directly analyzed without reduction. The reduced and nonreduced digests were analyzed on an LC−MS system composed of an HPLC (2690 Alliance Separations Module), a 2487 dual-wavelength UV detector, and an LCT mass spectrometer (Waters Corp., Milford, MA). The HPLC was equipped with a 1.0 mm × 250 mm YMC C_{18} column (AA12S052501WT) or a 1.0 mm × 250 mm Vydac C_{18} column (218TP51). Peptides were eluted with a 200 min gradient (from 0 to 70% acetonitrile) in 0.03% trifluoroacetic acid (TFA) at a flow rate of 0.07 mL/min. The temperature was 30 °C.

Endoprotease Asp-N Digestion and Separation of Digested Disulfide-Linked Peptides. The peak containing the disulfide-linked peptides in the LRRCT and stalk region on the tryptic peptide map was collected, dried under vacuum, and resuspended in 10 μL of a solution containing 0.1 M Tris-HCl (pH 6.5) and 1 mM $MgCl_2$. Approximately 0.02 μg of endoprotease Asp-N (endo-Asp-N, Sequencing Grade, Roche) was added to 0.6 μg of the peptides, after which the solution was incubated at room temperature for 6 h. The digest was analyzed on a nano-flow LC−MS system composed of a nano-flow HPLC (NanoAcquity, Waters Corp.) and a Q-TOF Premier mass spectrometer (Waters Corp.). The sample cone voltage was 35 V. A 0.10 mm × 100 mm Atlantic dC_{18} column (186002831, Waters Corp.) was used for the separation with a 50 min gradient (from 0 to 70% acetonitrile) in 0.1% formic acid at a flow rate of 400 nL/min. The column temperature was maintained at 35 °C.

Desialation, Endoprotease Glu-C Digestion, and LC−MS Analysis of the O-Linked Peptide, T34. The peak containing the tryptic glycopeptide T34 (residues 378−414) was collected, and ∼0.1 μg of the peptide was dried under vacuum and resuspended in 10 μL of PBS. To remove sialic acids, an aliquot of 0.5 μL of sialidase (10 milliunits/μL, Boehringer Mannheim) was added, after which the solution was incubated at room temperature for 20 h. Endoprotease Glu-C (endo-Glu-C, sequencing grade, Roche) digestion was carried out by treating the glycopeptide with 0.05 μg of the enzyme at room temperature for 24 h. The sialidase-treated tryptic peptide T34 was analyzed on a Voyager STR mass spectrometer (Applied Biosystems, Foster City, CA) using DHB as matrix. The endo-Glu-C digest of desialated T34 was analyzed on a nano-flow LC−MS system as described above.

Partial Reduction and Alkylation of the Disulfide-Linked Peptides. The disulfide-linked tryptic peptides were partially reduced using tris(2-carboxyethyl)phosphine hydrochloride (TCEP, Pierce) in 0.1 M citrate buffer (pH 3) containing 6 M guanidine HCl (*17*). Various amounts of TCEP were added to the solution to determine optimal conditions. The optimal amounts of TCEP were found to be 5 nmol for 20 pmol of the disulfide-linked peptides in the LRRNT region and 5 nmol for 10 pmol of the disulfide-linked peptides in the LRRCT and stalk regions. The total volume of the solution was 2.5 μL. The reduction was carried out at 37 °C for 15 min and was stopped by alkylating the partially reduced peptides with an excess of *N*-ethylmaleimide (NEM, Pierce) in 0.4 M citrate buffer (pH 4.5) containing 6 M GuHCl. The final concentration of NEM in the solution (5 μL) was 10 mM; the solution was kept at 37 °C for 1 h. The partially reduced and NEM-alkylated peptides were analyzed on a nano-flow LC−MS/MS system as described above, either directly or after further fractionation on a 2690 Alliance Separations Module with a 1.0 mm × 15 cm Atlantic dC_{18} column (186001283, Waters Corp.). A 70 min gradient (from 5 to 70% acetonitrile) in 0.1% TFA at a flow rate of 0.07 mL/min was used for fractionation, and the temperature was 30 °C.

Identification of Peptides by Mass Spectrometry. Components in peaks on the peptide maps were identified using MassLynx 4.0 software (Waters Corp.). MS/MS spectra were acquired using the data-dependent acquisition function (DDA) on a nano-flow LC−MS/MS system as described above. Ramped collision energy of 21−40 eV was used for MS/MS experiments, and MS/MS spectra were collected in the *m*/*z* range of 50−1800, with sampling every 0.5 s and a 0.05 s separation between consecutive spectra. The MS or MS/MS spectra acquired from the Q-TOF Premier mass spectrometer were deconvoluted by the MaxEnt 3 program that deconvolutes mutiple *m*/*z* peaks to a single MH^+ peak. Peptides linked by disulfide bonds were further identified by comparing the map of the nonreduced digest with the map of the corresponding reduced sample.

Modeling the Three-Dimensional (3D) Structure of NgR1-(344). The 3D model of human NgR1(344) was built with O version 8 (*18*) using the coordinates of human NgR1(310) as a template [PDB entry 1p8t (*14*)]. Residues 310−344 were built by hand on the basis of the constraints provided by the disulfide linkages between Cys-266 and Cys-335 and between Cys-309 and Cys-336, the locations of glycines and prolines in the strand kink, secondary structure predictions of α-helical regions, and the location of oppositely charged side chains on the convex surface of NgR1. The structure-based similarity between NgR1(310) (PDB entry 1p8t) and glycoprotein 1bα bound to thrombin [PDB entry 1p8v (*19*)] was used as a guide to model the loop of residues 310−334. Secondary structures of residues 310−348 were predicted using the "probabilistic discrete state-space models (*20*) (PSA server)" program which predicts a strong α-helix propensity for residues 323−328 (RATDEE) and residues 339−348 (DAADKASVLE). The geometry of the backbone chain was constrained by selecting similar fragment structures from the fragment database using the Lego ca command in O.

RESULTS

Purity and Bioactivity of NgR1 Proteins. Soluble full-length human NgR1 lacking the GPI linkage site (FL-NgR1, residues 27−438, Figure 1) of human NgR1 was expressed in CHO cells and purified by sequential chromatography. SDS−PAGE indicated that the purity of FL-NgR1 was greater than 90% with an average molecular mass of ∼65 kDa (Figure 2A). On SEC, the protein eluted as a single peak with a mass of ∼80 kDa (Figure 2B). The protein was tested for binding function in the ELISA format, and found to bind LINGO-1, OMgp, Nogo-66, p75, and TAJ equally well or better than the truncated versions containing the LRR region alone (see ref *10* for binding studies for p75 and TAJ). The titration data for p75 and TAJ highlight the contribution of the stalk region to coreceptor binding. A 10-fold higher affinity was seen for the FL-NgR1 compared with the truncated version NgR1(310) containing just the LRR region (*10*). Further analysis of function, in a competition ELISA using an anti-NgR1 antibody 14D5 (Fab) to block the binding

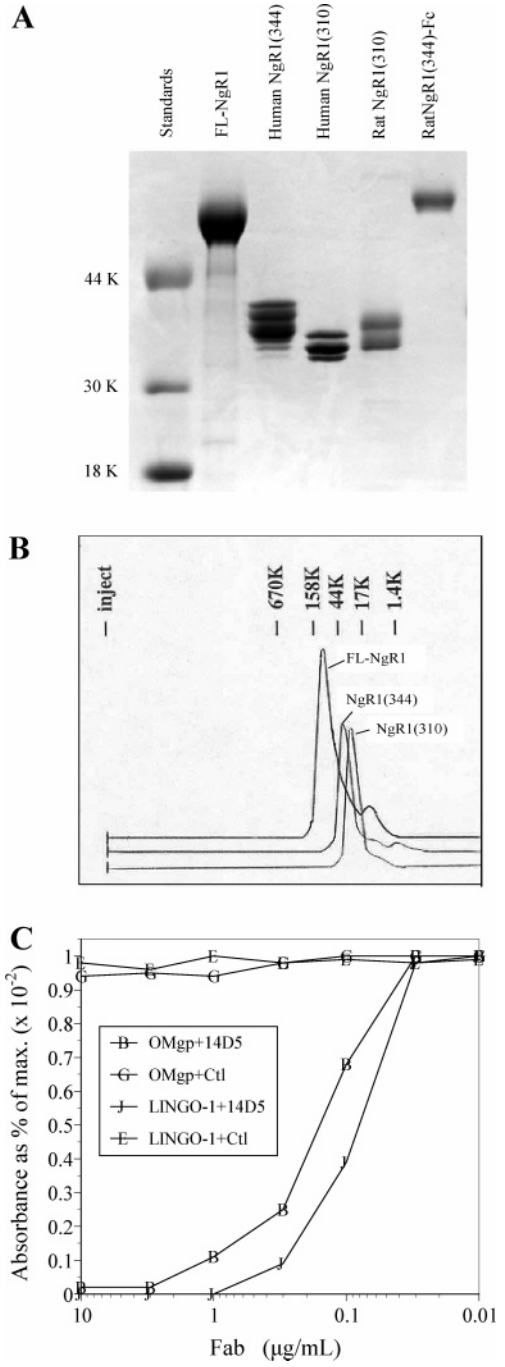

FIGURE 2: Characterization of the biochemical properties of FL-NgR1. (A) SDS−PAGE analysis of various NgR1 proteins (6 μg per lane). The gel was stained with Coomassie Blue R250. The multiple bands seen for human NgR1(344), human NgR1(310), and rat NgR1(310) are due to glycosylation heterogeneity. (B) Size exclusion chromatography (SEC) profiles for FL-NgR1, NgR310, and NgR344. (C) ELISA using anti-NgR1 antibody 14D5 Fab to block the binding of AP-OMgp and AP-Lingo-1 to FL-NgR1. Plates were coated with FL-NgR1 and then treated with AP-LINGO-1 or AP-OMgp either in the presence or in the absence of 14D5 Fab or a control Fab, following previous published protocols (*10*). The *Y*-axis shows the binding efficiency as a percentage of the maximum absorbance at 405 nm.

of AP-OMgp and AP-Lingo-1 to NgR1, verified the activities of FL-NgR1. As shown in Figure 2C, FL-NgR1 bound efficiently to both LINGO-1 and OMgp, and this binding could be inhibited by the anti-NgR1 antibody 14D5 (Fab), not a control Fab.

Analysis of the Amino Acid Sequence of the Full-Length Human NgR1 Protein. The amino acid sequence of FL-NgR1 was confirmed by tryptic peptide mapping on a LC−MS system. The peptide mapping was carried out on protein samples with and without PNGase F treatment. Trypsin was chosen as the cleavage enzyme for disulfide bond linkage studies since it was expected to generate the simplest set of Cys-containing peptides. Digestions were performed at pH 6.5 to minimize disulfide exchange. To overcome the problem of the lower rate of hydrolysis by trypsin at pH 6.5, the proteins were treated with endoprotease Lys-C before trypsin cleavage. The peptides were separated on a C_{18} reverse phase column and detected with an on-line ESI-TOF mass spectrometer. All significant peaks were identified and accounted for 97% of the predicted NgR1 sequence (Table 1). Undetected in the peptide maps were small and hydrophilic peptides that presumably coelute with the solvent peak. In the identified peptides, eight unexpected sites of post-translational modification were found: hydroxylation at Pro-352 (~75%; the peak elutes at 51.5 min in Figure 3 and is designated T31⟨Hyp-352⟩ in Table 1) and O-linked glycosylation at seven sites in peptide T34 (residues 378−414, Table 1). The hydroxylation site was identified by a MS/MS sequencing experiment on the 1652.9 Da peptide (data not shown). The glycosylation sites within peptide T34 were determined by mass spectrometric analysis of the endo-Glu-C digest of sialidase-treated T34 (data not shown), which shows that the N-linked glycosylation site, Asn-380, in T34 is not occupied but that all four Ser and three Thr residues in the peptide are glycosylated to some degree. The peptide contains, mainly, a total of four to six O-linked glycans (data not shown). Analytical results are consistent with predictions made using NetOGlyc version 3.1.

Analysis of Free Cys and Disulfide-Linked Cys Residues in Human NgR1 Protein. To directly assess which of the Cys residues in the mature structure were free, a tryptic digest of the pyridylethylated, nonreduced FL-NgR1 was analyzed on a LC−MS system after the digest had been reduced with DTT. Because the native protein was alkylated with 4-vinylpyridine prior to enzymatic cleavage, any Cys residues in the free thiol state should have been pyridylethylated, resulting in a 105 Da mass increase for each alkyl group. On the other hand, Cys residues involved in disulfide bonds should be detected as free cysteine, i.e., having a free thiol group after reduction. FL-NgR1 contains 14 Cys residues: four in the LRRNT region, two in the LRRs, four in the LRRCT region, and four in the CT stalk. All of the predicted cysteine-containing peptides in the tryptic peptide map of the reduced digest were identified, except for those containing Cys-80 and Cys-429, which, being small, presumably eluted with the solvent peak and were not analyzed. The bottom panel of Figure 3 shows the tryptic peptide maps for the pyridylethylated FL-NgR1 after reduction. All identified peptides are listed in Table 1 with cysteine-containing peptides in bold. Analysis of these data showed that 11 of the 12 identified Cys residues were in the free thiol form after reduction, and that Cys-140 in peptide T10 (residues 140−151) was pyridylethylated. Therefore, we can infer that 12 of the Cys residues in native FL-NgR1 are involved in six disulfide bonds and two are unpaired. Moreover, utilizing information from the crystal structure of NgR1(310) (*14*, *15*), one can predict that Cys-80 exists as a free thiol, since in

Table 1: LC−MS Analysis of Peptides from a Tryptic Digest of Reduced and Pyridylethylated FL-NgR1

tryptic peptide[a]	residue numbers	retention time (min)	observed molecular mass (Da)[b]	calculated molecular mass (Da)[b]
T1	Leu and 27−38[c]	57.7	1395.68	1395.60
T2	39−61	67.9	2307.22	2307.20
T3	62−68	43.6	855.49	855.47
T4	69−78	50.6	1083.59	1083.58
PE-T5	79−81		N/D	245.15
T6 + $Hex_5HexNAc_4Fuc$[d]	82−95	96.7	3417.67	3417.58
T6	82−95	108.4	1648.94	1648.94
T6 (deglycosylated)	82−95	111.6	1649.92	1649.95
T7	96−119	147.9	2557.38	2557.34
T8	120−131	57.9	1255.64	1255.63
T9	132−139	50.6	1003.54	1003.56
PE-T10	140−151	79.2	1393.81	1393.72
T11	152−175	133.1	2708.52	2708.38
T12 + $Hex_5HexNAc_4Sia_{1-2}Fuc$[d]	176−189	85.4	3374.47	3374.48
			3665.68	3665.58
T12 (deglycosylated)	176−189	99.2	1606.82	1606.85
T13	190−196	31.4	786.44	786.42
T14	197−199		not detected	393.23
T15	200−206	34.9	796.45	796.42
T16	207−213	41.8	892.55	892.52
T17	214−217	42.0	1169.64	1169.62
T18	224−227	14.9	460.26	460.25
T19′ (deglycosylated)	233−250	116.8	1911.12	1911.07
T19 (deglycosylated)	228−250	168.3	2532.42	2532.39
T19 + $Hex_5HexNAc_4SiaFuc_{0-1}$[d]	228−250	146.2	4447.0	4447.8
			4594.0	4593.9
T20	251−256	50.6	762.45	762.44
T21	257−267	65.1	1333.55	1333.55
T22	268−277	92.9	1267.72	1267.72
T22′	270−277	95.4	1040.59	1040.58
T23−T24	278−292	56.1	1648.80	1648.80
T24	280−292	52.0	1345.63	1345.63
T25	293−296	17.9	416.23	416.26
T26−T27	297−300	34.8	531.34	531.33
T28	301−323	80.6	2410.18	2410.19
T29	324−334	57.1	1168.61	1168.60
T30	335−343	22.5	949.41	949.36
T31⟨Hyp-352⟩	344−360	51.5	1652.89	1652.89
T31	344−360	54.4	1636.90	1636.89
T32−T33 (deglycosylated)	361−377	36.2	1603.78	1603.80
T33 (deglycosylated)	363−377	34.9	1390.64	1390.67
T34 + 4−6 O-linked glycans[d] (HexNAcHex)[e]	378−414	65.8	5228.28	5228.38
			5593.41	5593.52
			5958.57	5958.64
T35−T36	415−421	17.9	830.45	830.43
T37	422		not detected	146.11
T38	423−424		not detected	288.15
T39	425−426		not detected	275.16
T40	427−430		not detected	501.21
T41	431−438	16.5	645.32	645.31

[a] T designations denote predicted tryptic peptides from the FL-NgR1 sequence where T1 is the N-terminal peptide and T41 is the C-terminal peptide. Cys-containing peptides are in bold. Deglycosylated peptides were identified in a tryptic peptide map of PNGase F treated pyridylethylated FL-NgR1 (figure not shown). [b] Monoisotopic masses except for those of glycopeptides T34 and T39. [c] Leu is from the Flag tag at the N-terminus of FL-NgR1. [d] Only major components are listed. [e] The fraction was treated with sialidase prior to mass spectrometric analysis.

the crystal structure it is buried in the LRR region. By inference, Cys-429 in the CT stalk region, which is absent in the crystal structure, must be involved in disulfide bond formation.

Analysis of Disulfide Linkages in the FL-NgR1 Protein. Disulfide structures within NgR1 were determined by analyzing peptide maps of nonreduced digests. On the basis of the disulfide structure seen in the crystal structure of NgR1(310) (*14*, *15*), the nonreduced digest should contain two groups of disulfide-linked peptides, one from the LRRNT region and the other from the LRRCT region. In fact, analysis of the peptide map of the nonreduced digest did reveal a group of disulfide-linked peptides (T1/T2) from the LRRNT region eluting at 74.3 min (Figure 3, top panel). Mass spectrometric analysis of the peak showed that it contains two peptides, T1 (residues 27−38) and T2 (residues 39−61), linked by two disulfide bonds (observed mass of 3698.77 Da, calculated mass of 3698.77 Da; Table 2). The peak containing T1/T2 disappeared when the digest was reduced with DTT, and concomitantly, on the reduced map, two new peaks corresponding to the individual peptides, T1 and T2 (Figure 3, bottom panel), were observed. Peptide T1 contains three cysteines. Due to the lack of a protease that can cleave between Cys-27 and Cys-29 and between Cys-29 and Cys-33, the exact disulfide linkages in T1/T2 had to be determined by partial reduction with TCEP and alkylation

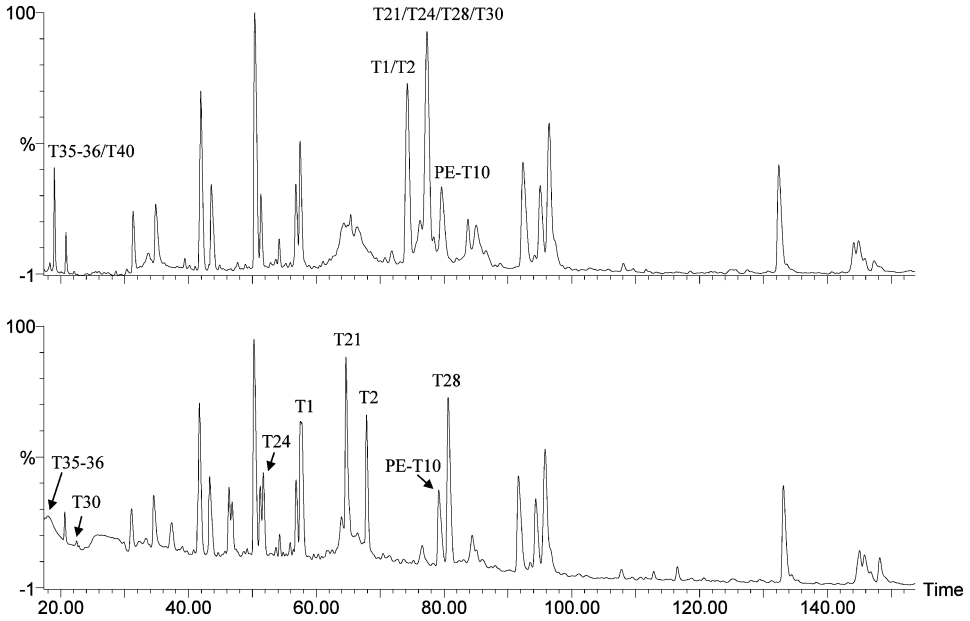

FIGURE 3: Tryptic peptide maps of pyridylethylated FL-NgR1. Digests were separated by HPLC on a YMC C_{18} column and analyzed on-line with an LCT mass spectrometer: (top) nonreduced digest and (bottom) reduced digest. Identified peak characteristics are summarized in Table 1.

Table 2: Disulfide-Linked Peptides Detected in a Tryptic Peptide Map of the Nonreduced Digest of Pyridylethylated FL-NgR1

disulfide-linked tryptic peptide[a]	residue numbers	retention time (min)	observed molecular mass (Da)[b]	calculated molecular mass (Da)[b]
T1/T2 with two disulfide bonds	Leu and 27−38[c] 39−61	74.3	3698.77	3698.77
T21/T24/T28/T30 with three disulfide bonds	257−267 280−292 301−323 335−343	77.3	6032.62	6032.68
T35-T36/T40 with one disulfide bond	415−421 427−430	19.0	1329.62	1329.62

[a] T designations denote predicted tryptic peptides from the FL-NgR1 sequence where T1 is the N-terminal peptide and T41 is the C-terminal peptide. [b] Monoisotopic masses. Corresponding observed and calculated average masses for T21/T24/T28/T30 are 6036.67 and 6036.72 Da, respectively. [c] Leu is from the Flag tag at the N-terminus of FL-NgR1.

with NEM followed by LC−MS/MS analysis. From the NgR1(310) crystal structure (*14*, *15*), we can infer that T1 will have an intrapeptide disulfide bond and is linked to T2 by an interpeptide disulfide bond. Mass spectrometric analysis of the products of the partial reduction and alkylation, after separation on a C_{18} column, detected the following predicted partially reduced, NEM-alkylated peptides: T1 containing one disulfide bond and one *N*-ethylsuccinimidyl (NES) group (observed MH^+ of 1519.64 Da, calculated MH^+ of 1519.64 Da), T2 with one NES group (observed MH^+ of 2433.26 Da, calculated MH^+ of 2433.25 Da), and T1/T2 containing one interpeptide disulfide bond and two NES groups (observed MH^+ of 3951.90 Da, calculated MH^+ of 3951.89 Da). The MS/MS spectrum for T1 containing one disulfide bond and one NES group, shown in Figure 4, indicates that the NES group is on Cys-29 [internal fragment ions, PGAC(NES) and PGAC(NES)V, y_{11}-related ions, Figure 4], which means that Cys-33 is linked to Cys-27 by an intrapeptide disulfide bond and that Cys-29 is linked to Cys-43 in T2 by an interpeptide disulfide bond. MS/MS sequencing results for T1/T2 containing one interpeptide disulfide bond and two NES groups are consistent with this conclusion, since analysis showed that the two NES groups were at Cys-27 and Cys-33 (data not shown).

The crystal structure of the LRRCT region of NgR1(310) (*14*, *15*) revealed disulfide linkages of Cys-264 to Cys-287 and Cys-266 to Cys-309. Therefore, the four Cys residues in the LRRCT region should be contained in three tryptic peptides [T21 (residues 257−267), T24 (residues 280−292), and T28 (residues 301−323)] linked together by two interpeptide disulfide bonds (the calculated mass for this cluster should be 5088.68 Da). The three individual peptides, T21, T24, and T28 (bottom panel of Figure 3 and Table 1), were easily identified in the map of the reduced digest, but no significant peak corresponding to this peptide cluster, T21/T24/T28, was found in the map of the nonreduced digest. Instead, a prominent peak having a monoisotopic mass of 6032.62 Da occurred, which corresponds to a four-peptide cluster containing T21, T24, T28, and T30 (residues 335−343) linked by three disulfide bonds (calculated monoisotopic mass of 6032.68 Da; top panel of Figure 3 and Table 2). Since peptides T21 and T30 each contain two Cys residues, one Cys in peptide T21 must form a disulfide bond with one in peptide T30, although the exact linkages could not be determined. The tryptic peptide mapping analysis also showed that the peak at 19.0 min contains the other two Cys-containing peptides in the CT stalk region, and that they are linked by a disulfide bond between Cys-419 and Cys-429 (Table 2 and Figure 3, top panel).

To determine disulfide linkages in the peptide T21/T24/T28/T30 complex, the peak was collected and further cleaved by endo-Asp-N followed by mass spectrometric analysis on a nano-flow LC−MS system. Two significant components were detected by mass spectrometric analysis in the nonreduced digest (data not shown). A detected MH^+ of 2076.89 Da (Figure 5) for the first component matches the calculated

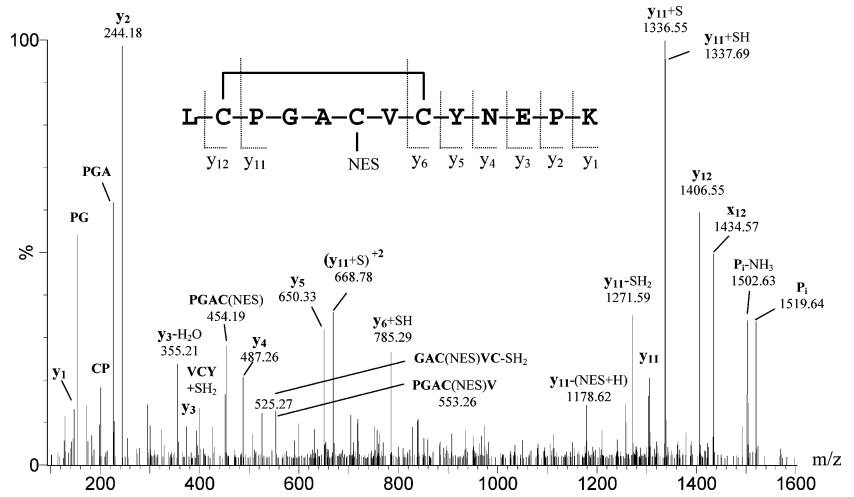

FIGURE 4: MS/MS spectrum of partially reduced tryptic peptide T1 containing a NES group. The sequence of the peptide, the fragmentation pattern, and detected fragment ions are shown at the top of the panel. y designates ions that contain the C-terminal region of the peptide with one or more amino acid residues generated by collision-induced dissociation (CID). S, SH, and SH_2 designate a sulfur atom from the side chain of Cys, with no, one, and two protons, respectively. Calculated masses for some critical ions are as follows: $y_2 = 244.17$, $y_3 = 373.21$, $y_4 = 487.25$, $y_5 = 650.31$, $y_6 + SH = 785.30$, $y_{11} - SH_2 = 1271.57$, $y_{11} + S = 1336.53$, $y_{11} + SH = 1337.53$, $y_{12} = 1406.55$, internal fragment ions PGAC(NES) = 454.18, GAC(NES)VC $- SH_2 = 525.21$, PGAC(NES)V = 553.24, and precursor ion $P_i = 1519.64$.

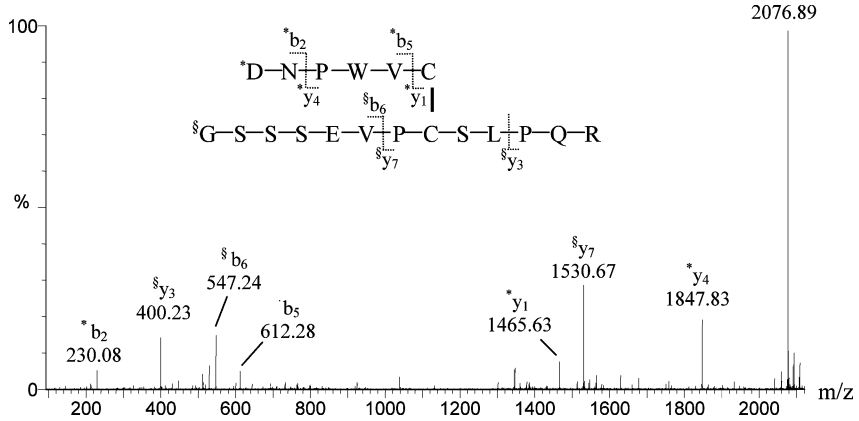

FIGURE 5: Deconvoluted mass spectrum for one of the two major components detected in the endo-Asp-N-treated disulfide-linked tryptic peptide cluster T21/T24/T28/T30 from FL-NgR1. The sequences of the peptides, fragmentation patterns, and detected fragment ions are shown at the top of the panel. y ions containing the C-terminal region of the peptide and b ions containing the N-terminal region of the peptide were generated by in-source fragmentation. Calculated masses are as follows: $*b_2 = 230.08$, $*b_5 = 612.28$, $*y_1 = 1465.64$, $*y_4 = 1847.84$, $^{\S}b_6 = 547.24$, $^{\S}y_3 = 400.23$, $^{\S}y_7 = 1530.68$, and the intact disulfide-linked peptide cluster = 2076.91.

MH^+ of 2076.91 Da for peptide T21 and peptide T24 linked by a disulfide bond between Cys-264 and Cys-287, as seen in the crystal structure of NgR1(310). The identity of this fragment was confirmed by the observation of in-source fragmentation ions (Figure 5). The observed MH^+ of 2879.22 Da for the other component matches the calculated MH^+ of 2879.25 Da for the group of three peptides, residues 265−267 (derived from T21), residues 305−323 (derived from T28), and residues 335−338 (derived from T30), linked by two interpeptide disulfide bonds, which indicated that Cys-266 and Cys-309 in the LRRCT region form disulfide bonds with Cys-335 and Cys-336 in the CT stalk region somehow (data not shown). Determination of the exact disulfide pairings, Cys-266 and Cys-309 with Cys-335 and Cys-336, in this case, was complicated by the fact that no reagents exist that can cleave the backbone between Cys-335 and Cys-336.

The disulfide pairing arrangement in the T21/T24/T28/T30 complex was further elucidated by subjecting it to partial reduction with TCEP followed by alkylation with NEM and analysis by nano-flow LC−MS. Figure 6 shows the nano-flow LC−MS results (TIC), and Table 3 lists the identities of the components in the peaks. The doublet peaks seen for certain peptides are due to stereoisomers generated by NEM alkylation. The MS/MS spectra are the same for individual peaks in each doublet (data not shown). The doublet peak containing T28/T30 with a disulfide bond and an NES group was collected from a fractionation run on a 1 mm × 150 mm column, and further analyzed on a nano-LC−MS/MS system after it had been fully reduced with DTT. Figure 7

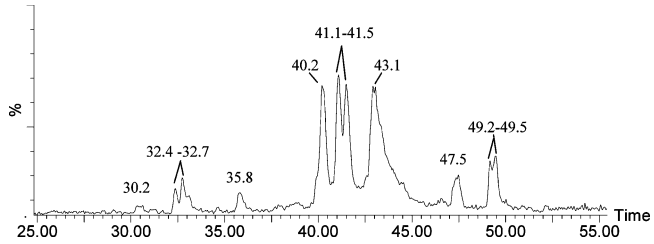

FIGURE 6: Total ion chromatogram (TIC) of partially reduced, NEM-alkylated disulfide-linked peptide cluster T21/T24/T28/T30 from FL-NgR1. Identities of components in each peak are listed in Table 3.

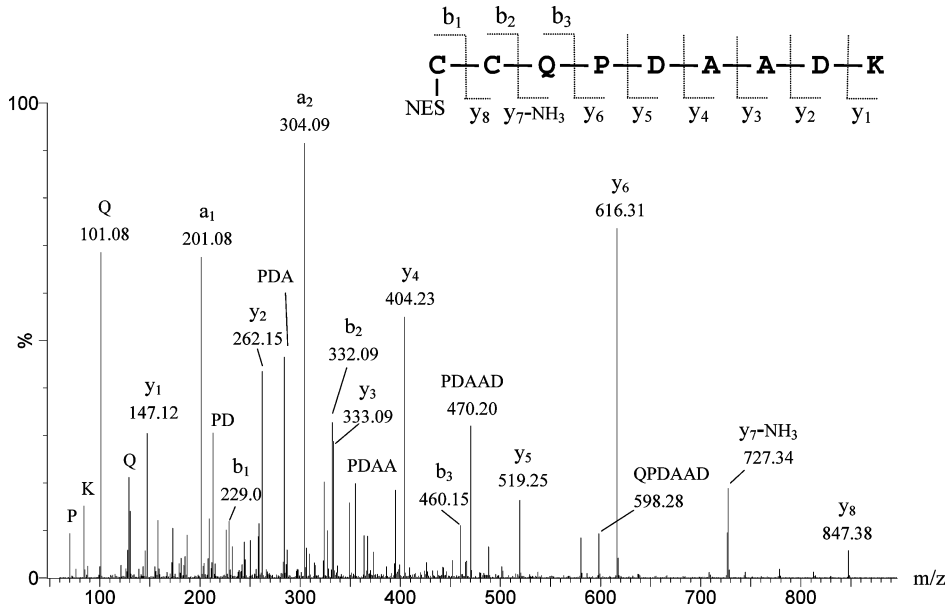

FIGURE 7: MS/MS spectrum of the partially reduced, NEM-alkylated peptide T30. The peptide contains residues 335−343 with a NES group and was generated from reduction of partially reduced, NEM-alkylated, and disulfide-linked tryptic peptides T30 (residues 335−343) and T28 (residues 301−323). The sequence of the peptide, the fragmentation pattern, and detected fragment ions are shown at the top of the panel. y and b ions are as described for Figure 5, and a ions reflect fragmentation due to loss of a carbonyl from corresponding b ions. Calculated masses are as follows: $a_1 = 201.07$, $b_1 = 229.06$, $a_2 = 304.08$, $b_2 = 332.07$, $b_3 = 460.13$, $y_1 = 147.11$, $y_2 = 262.14$, $y_3 = 333.18$, $y_4 = 404.21$, $y_5 = 519.27$, $y_6 = 616.29$, $y_7 - NH_3 = 727.33$, $y_8 = 847.36$, and the intact peptide = 1074.41.

Table 3: LC−MS Analysis of Components from the Partially Reduced, NEM-Alkylated Peptide Cluster T21/T24/T28/T30

tryptic peptide[a]	retention time (min)	observed molecular mass (Da)[b]	calculated molecular mass (Da)[b]
T30 with two NES	30.4	1199.58	1199.46
T24 with one NES	32.4−32.8	1470.70	1470.68
T21/T24/T30 with one NES	35.8	3749.56	3749.56
T21/T24 with one NES	40.25	2802.21	2802.22
T28/T30 with one NES	41.1−41.5	3482.57	3482.58
T21/T24/T28/T30	43.0	6032.65	6032.68
T21 with two NES	47.4	1583.66	1583.65
T28 with one NES	49.2−49.5	2535.26	2535.23

[a] T designations denote predicted tryptic peptides from FL-NgR1 sequence where T1 is the N-terminal peptide and T41 is the C-terminal peptide. NES is the *N*-ethylsuccinimidyl group resulting from alkylation by NEM. [b] Monoisotopic masses.

shows the MS/MS spectrum of peptide T30 containing a NES group. Both b_1 and y_8 ions, detected by MS/MS sequencing, show that the NES group is at Cys-335, not Cys-336, because the observed *m*/*z* value is 229.08 for b_1 and 847.38 for y_8 (the calculated *m*/*z* value is 229.06 for b_1 and *m*/*z* 847.36 for y_8, if Cys-335 is alkylated with NEM; the calculated *m*/*z* value is 104.10 for b_1 and 972.46 for y_8, if Cys-336 is alkylated with NEM), which indicates that Cys-336 forms a disulfide bond with Cys-309. Consequently, then, Cys-335 must be linked to Cys-266.

Analysis of the Disulfide Structures of NgR1 Proteins Made from Different Constructs. Disulfide structures in human NgR1(310) protein, human NgR1(344) protein, rat NgR1(310) protein, and rat NgR1(344)−rat Fc(IgG1) fusion protein [rat NgR1(344)−Fc] were also analyzed by tryptic peptide mapping. The results are summarized in Table 4. In all cases, the observed disulfide structures within the LRRNT region were identical and as predicted. In contrast, two different patterns were observed for the disulfide linkages in the LRRCT, one identical to the pattern observed in FL-NgR1 and the other identical to the pattern seen in the crystal structure of NgR1(310). For example, a large peak with an average mass of 6036.21 Da was detected on the peptide map of the nonreduced human NgR1(344). This corresponds to the four-peptide T21/T24/T28/T30 cluster linked by three disulfide bonds (calculated average mass of 6036.72 Da, Table 4), the same as that seen on the peptide map of the unreduced FL-NgR1 (observed average mass of 6036.67 Da in FL-NgR1, Tables 2 and 4). On the other hand, the peptide map of human NgR1(310) shows a peak with a mass of 3892.45 Da that matches that for the disulfide-linked peptide T21/T24/T28 cluster (calculated mass of 3892.73 Da), as predicted from the crystal structure of NgR1(310). These analyses showed that disulfide structures in rat NgR1(310) and human NgR1(310) proteins which lack the two Cys residues, Cys-335 and Cys-336, in the CT stalk region are the same as those seen in the crystal structure of human NgR1(310), and that the disulfide structures in the rat NgR1-(344)−Fc and human NgR1(344) proteins which do have the two Cys residues in the CT stalk region are the same as those seen in FL-NgR1.

A Three-Dimensional Model of the NgR1(344) Protein. Glycoprotein 1bα is a platelet receptor that binds von Willebrand factor and thrombin, and like NgR1, it is an LRR protein with both N- and C-terminal cysteine-rich caps. Crystal structures for glycoprotein 1b have been determined in the absence and presence of its ligands. On the basis of the crystal structures of NgR1(310) [PDB entry 1p8t (*14*)], glycoprotein 1bα bound to thrombin [PDB entry 1p8v (*19*, *21*)], and our experimentally determined disulfide structure in the LRRCT and CT stalk regions of FL-NgR1, we constructed the three-dimensional model of human NgR1-(344) as shown in Figure 8. The region containing residues 27−309 of NgR1 was built using the published coordinates

Table 4: Summary of Mass Spectrometric Analyses for Disulfide Structures in NgR1 Proteins Made from Different Constructs

disulfide-linked peptides[a]	observed molecular mass (Da)				calculated molecular mass (Da)
	NgR1(310)	NgR1(344)	rat NgR1(310)	rat NgR1(344)−Fc	
T1/T2[b] with two disulfide bonds (human)	3672.63	3672.76			3672.72 (human)
T1/T2[b] with two disulfide bonds (rat)			3603.67	3603.64	3603.65 (rat)
T21/T24/T28 (human) with two disulfide bonds	3892.45	not detected			3892.73 (human)
T18/T21/T25 (rat) with two disulfide bonds			3591.69	not detected	3591.60 (rat)
T21/T24/T28/T30 (human) with three disulfide bonds	not appropriate	6036.21[c]			6036.72 (human)[c]
T18/T21/T25/T26 (rat) with three disulfide bonds			not appropriate	7240.51[c]	7241.06 (rat)[c]

[a] T designations denote predicted tryptic peptides from the FL-NgR1 sequence where T1 is the N-terminal peptide and T41 is the C-terminal peptide. Due to differences in their primary sequences, T18, T21, T25, and T26 in rat correspond to T21, T24, T28, and T30 in human, respectively. [b] T1 for NgR1(310) and NgR1(344) contains a Ser from the signal peptide at the N-terminus of the proteins. [c] Average masses. Corresponding calculated monoisotopic masses are 6032.68 and 7236.30 Da, respectively.

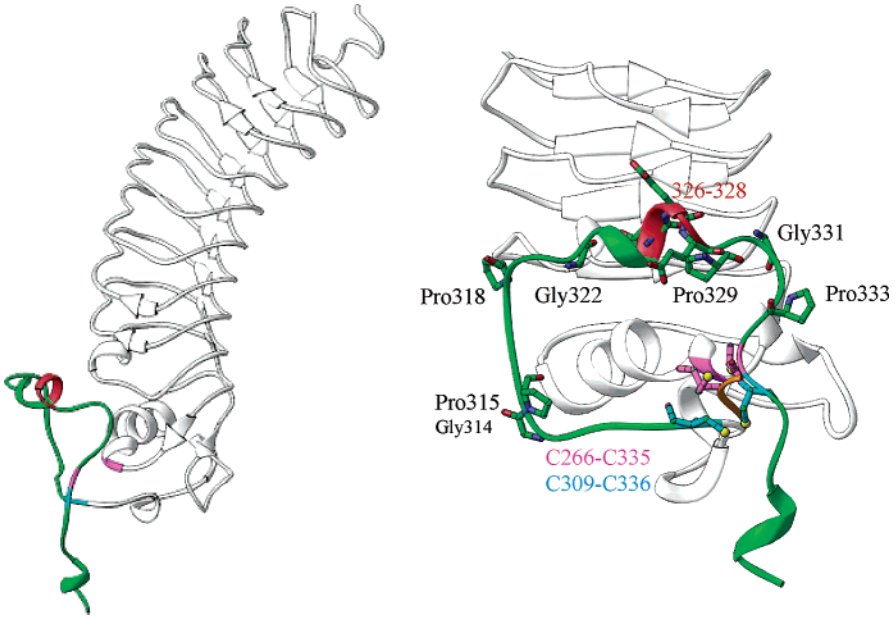

FIGURE 8: Three-dimensional model of the human NgR1(344) protein. The portion of model generated using the published structures of human NgR1(310) is colored gray (*15*), and that for the loop of residues 310−334 based on the structure of glycoprotein 1bα bound to thrombin is colored green (*19*). Cystines that constrain the loop of residues 310−334 are colored magenta (Cys-266 and Cys-335) and blue (Cys-309 and Cys-336); residues 326−328, which comprise the acidic patch, are colored red, and Gly and Pro residues are colored green.

of NgR1(310) [PDB entry 1p8t (*14*)]. An in-house crystal structure of rat NgR1(310/312), generated by papain cleavage of rat NgR1(344)−Fc, showed that the overall structure of rat NgR1(310/312) is the same as the published structure of human NgR1(310), except that the thiol groups of the second and fourth Cys residues (Cys-266 and Cys-309) in the LRRCT region of rat NgR1(310/312) are in the free thiol form (data not shown). The region comprising residues 310−334 was built using the partially ordered anionic tail of glycoprotein 1bα bound to thrombin I (*19*, *21*) as a template. In this structure, thrombin binds to the C-terminal tail of glycoprotein 1bα as well as to the convex surface of the LRR domain. The NgR1 model shows that a loop containing residues 310−334 appears near the convex surface of the Nogo receptor forming part of the LRRCT domain. This region of NgR1 is far from the concave side that is required to interact with myelin ligands (*14*, *15*). Residues 337−344 extend away from the Nogo-310 domain due to the constraints of the disulfide bonds between Cys-265 and Cys-335 and between Cys-309 and Cys-336. From the available data, we cannot determine whether the loop containing residues 310−334 of the NgR1 (310−334 loop) is freely mobile or associated with the convex side of the LRRs or LRRCT region. The model was built to place a negatively charged patch (residues Asp-326, Glu-327, and Glu-328), which is conserved in the rat, human, and mouse NgR1 sequences, close to His-218 on the convex side of the eighth LRR in order to favor charge−charge interaction.

DISCUSSION

We have used peptide mapping in conjunction with mass spectrometry to accurately determine the disulfide linkages in the LRRCT and CT stalk regions of FL-NgR1. These studies show that Cys-264 is linked to Cys-287, Cys-266 to Cys-335, Cys-309 to Cys-336, and Cys-419 to Cys-429. In studying the disulfide structure in NgR1, we discovered ambiguities in the disulfide linkages drawn from crystallographic data for a truncated fragment of NgR1 that terminated at the predicted C-terminus of the LRRCT sequence. To reconcile these differences, we characterized four other recombinant varieties of NgR1: rat and human NgR1(310), analogous to the forms that had been crystallized, and rat and human NgR1(344), which contain the two cysteines in the stalk. When NgR1(310) was analyzed, we indeed observed the Cys-266−Cys-309 linkage as seen in the crystal structure. However, when NgR1(344) was char-

acterized, we observed in it the alternate pairing structure. These findings suggest that the Cys-266−Cys-309 linkage seen in NgR1(310) is caused by the truncation and is not representative of the structure found in the intact protein.

The LRR C-terminal cap (LRRCT) is conserved in many LRR proteins. The LRRCT region in NgR1 with its four Cys residues belongs to the CF1 type and is the most common type seen in extracellular LRR proteins (*22*−*24*). Crystal structures of glycoprotein 1bα and NgR1(310) (the only available crystal structures for CF1-type LRR proteins) showed that the first Cys in the LRRCT forms a disulfide bond with the third Cys and the second Cys with the fourth. These disulfide linkages were considered to be general for the CF1 type of C-flanking domain in other LRR proteins. However, our analysis of the disulfide structure in the LRRCT region of FL-NgR1 not only demonstrates that the predicted disulfide structure for the LRRCT region of NgR1 is incorrect but also identifies an alternative cysteine pairing structure.

To predict how these alternative disulfide linkages in the LRRCT and stalk regions of NgR1, revealed by our experiments, affect the overall folding of the LRRCT region of NgR1, we have built a three-dimensional structural model for NgR1(344) based on the crystal structure of NgR1(310) [PDB entry 1p8t (*14*)] and glycoprotein 1bα [PDB entry 1p8v (*19*)]. In this model, the 310−334 loop in the CT stalk region folds back to the convex side of the LRRs and the rest of the C-terminus of NgR1(344), residues 337−344, points away from the LRRs, due to constraints imposed by the disulfide linkages between Cys-266 and Cys-335 and between Cys-309 and Cys-336. This folding arrangement is not unique to NgR1. The crystal structure of the complex of glycoprotein 1bα with the von Willebrand factor A1 domain (vWF-A1) showed that a disordered loop (*β*-switch) protrudes from the LRRCT region into the concave face to participate in binding of the ligand, vWF-A1 (*25*), while the crystal structure of the complex of glycoprotein 1bα with thrombin showed that the post-LRRCT region (residues Asp-269−Tyr-279) of glycoprotein 1bα folds back to the convex side of the LRRs and binds to its ligand, thrombin, even though glycoprotein 1bα does not have Cys residues in the post-LRRCT region (*19*, *26*). A crystal structure of the complex between the ubiquitin−protein ligase components Skp1 and Skp2 also showed that the approximately 30-residue C-terminal tail of Skp2 is folded back along the concave side to its first LRR, where it has been proposed to participate in or to regulate substrate binding (*27*). More interestingly, the crystal structure of the third Slit LRR domain (containing five LRRs flanked by a LRRNT cap and a CF1 type of LRRCT cap) showed that its C-terminal tail folded onto the convex side by forming an additional disulfide bridge between a Cys residue in a segment just following the LRRCT region and a Cys at the end of the fourth LRR (*28*).

Several laboratories have shown that NgR1(310) alone is sufficient for binding to myelin ligands and coreceptors but that the stalk region enhances the interaction with coreceptors p75 and TAJ (*10*, *11*), and that the binding affinity of both p75 and TAJ to NgR1 is in the following order: FL-NgR1 > NgR1(344) > NgR1(310) (*10*). Our model of NgR1(344) reveals an anionic patch (residues 326−328) in the 310−334 loop that folds to the convex side of the LRRs. We believe that a portion of the 310−334 loop may play an important role in the interactions with the coreceptors LINGO-1, p75, and TAJ, which are necessary for signal transduction. Because the disulfide bond between Cys-309 and Cys-336 creates a loop that would not be stabilized by the disulfide linkage between Cys-266 and Cys-335, the disulfide bond formed between Cys-309 and Cys-336 could be a driving force for protein folding in the region containing residues 311−336. The importance of Cys-309 and Cys-366 could be tested by mutating them in NgR1(344) and testing the effects on coreceptor bindings. Moreover, although the binding affinity of NgR1(344) to p75 and TAJ is higher than that of NgR1(310), it is much lower than that of FL-NgR1-(310), indicating the importance of the function of the region containing residues 345−438 of NgR1. There is no information available about the three-dimensional structure of the CT stalk region of NgR1 yet, but one can predict that the orientation of the stalk will depend on correct disulfide formation of Cys-266 with Cys-335 and Cys-309 with Cys-336. The disulfide linkage between Cys-419 and Cys-429 will also presumably play an important role in stabilizing the structure of the very hydrophilic region (residues 345−438) that contains seven O-linked and two N-linked glycans and a hydroxyproline and consists mainly of random coils (predicted by the NNPredict secondary structure prediction program in Vector NTI Suite 7).

In summary, we have identified a novel disulfide structure in the LRRCT and stalk regions of NgR1. The studies have shown that the actual LRRCT domain is larger than that predicted (Figure 1). The three-dimensional model of NgR1-(344) indicates that the peptide comprising residues 310−334 folds back to the convex side of the LRRs of NgR1. We suggest that the 310−334 loop participates in the interactions with coreceptors of NgR1, such as LINGO-1, p75, and TAJ. Further structure and activity studies are needed to understand the NgR1/Lingo-1/p75 or NgR1/Lingo-1/TAJ signaling mechanism.

ACKNOWLEDGMENT

We thank Dr. Greg Thill for producing FL-NgR1, AP-LINGO-1, and AP-OMgp, Jessica Schauer, Betty Zheng, and Eugene Choi for producing the 14D5 Fab, Konrad Miatkowski, Joseph Amatucci, and Shelly McCullough for large scale fermentation, and Carmen Young for N-terminal sequencing.

REFERENCES

1. GrandPré, T., Nakamura, F., Vartanian, T., and Strittmatter, S. M. (2000) Identification of the Nogo inhibitor of axon regeneration as a Reticulon protein, *Nature 403*, 439−444.
2. Huber, A. B., and Schwab, M. E. (2000) Nogo-A, a potent inhibitor of neurite outgrowth and regeneration, *Biol. Chem. 381*, 407−419.
3. Prinjha, R., Moore, S. E., Vinson, M., Blake, S., Morrow, R., Christie, G., Michalovich, D., Simmons, D. L., and Walsh, F. S. (2000) Neurobiology: Inhibitor of neurite outgrowth in humans, *Nature 403*, 383−384.
4. Mukhopadhyay, G., Doherty, P., Walsh, F. S., Crocker, P. R., and Filbin, M. T. (1994) A novel role for myelin-associated glycoprotein as an inhibitor of axonal regeneration, *Neuron 13*, 757−767.
5. McKerracher, L., David, S., Jackson, D. L., Kottis, V., Dunn, R. J., and Braun, P. E. (1994) Identification of myelin-associated glycoprotein as a major myelin-derived inhibitor of neurite growth, *Neuron 13*, 805−811.

6. Wang, K. C., Koprivica, V., Kim, J. A., Sivasankaran, R., Guo, Y., Neve, R. L., and He, Z. (2002) Oligodendrocyte-myelin glycoprotein is a Nogo receptor ligand that inhibits neurite outgrowth, *Nature 417*, 941−944.
7. Fournier, A. E., GrandPré, T., and Strittmatter, S. M. (2001) Identification of a receptor mediating Nogo-66 inhibition of axonal regeneration, *Nature 409*, 341−346.
8. Niederöst, B., Oertle, V., Fritsche, J., McKinney, R. A., and Bandtlow, C. E. (2002) Nogo-A and myelin-associated glycoprotein mediate neurite growth inhibition by antagonistic regulation of RhoA and Rac1, *J. Neurosci. 22*, 10368−10376.
9. Yamashita, T., Higuchi, H., and Tohyama, M. (2002) The p75 receptor transduces the signal from myelin-associated glycoprotein to Rho, *J. Cell Biol. 157*, 565−570.
10. Shao, Z., Browning, J. L., Lee, X., Scott, M. L., Shulga-Morskaya, S., Allaire, N., Thill, G., Levesque, M., Sah, D., McCoy, J. M., Murray, B., Jung, V., Pepinsky, R. B., and Mi, S. (2005) TAJ/TROY, an orphan TNF receptor family member, binds Nogo-66 receptor 1 and regulates axonal regeneration, *Neuron 45*, 353−359.
11. Park, J. B., Yiu, G., Kaneko, S., Wang, J., Chang, J., and He, Z. (2005) A TNF receptor family member, TROY, is a coreceptor with Nogo receptor in mediating the inhibitory activity of myelin inhibitors, *Neuron 45*, 345−351.
12. Mi, S., Lee, X., Shao, Z., Thill, G., Ji, B., Relton, J., Levesque, M., Allaire, N., Perrin, S., Sands, B., Crowell, T., Cate, R. L., McCoy, J. M., and Pepinsky, R. B. (2004) LINGO-1 is a component of the Nogo-66 receptor/p75 signaling complex, *Nat. Neurosci. 7*, 221−228.
13. Sivasankaran, M. R., Segal, R., and He, Z. (2002) p75 interacts with the Nogo receptor as a co-receptor for Nogo, MAG and OMgp, *Nature 420*, 74−78.
14. He, X. L., Bazan, J. F., McDermott, G., Park, J. B., Wang, K., Tessier-Lavigne, M., He, Z., and Garcia, K. C. (2003) Structure of the Nogo receptor ectodomain: A recognition module implicated in myelin inhibition, *Neuron 38*, 177−185.
15. Barton, W. A., Liu, B. P., Tzvetkova, D., Jeffrey, P. D., Fournier, A. E., Sah, D., Cate, R., Strittmatter, S. M., and Nikolov, D. B. (2003) Structure and axon outgrowth inhibitor binding of the Nogo-66 receptor and related proteins, *EMBO J. 22*, 3291−3302.
16. Pepinsky, R. B. (1991) Selective precipitation of proteins from guanidine hydrochloride-containing solutions with ethanol, *Anal. Biochem. 195*, 177−181.
17. Burns, J. A., Bulter, J. C., Moran, J., and Whitesides, G. M. (1991) Selective reduction of disulfides by tris(2-carboxyethyl)phosphine, *J. Org. Chem. 56*, 2648−2650.
18. Jones, T. A., and Kjeldgaard, M. (1998) *Essential O software manual*, pp 178, Uppsala University, Uppsala, Sweden.
19. Dumas, J. J., Kumar, R., Seehra, J., Somers, W. S., and Mosyak, L. (2003) Crystal structure of the GpIbα-thrombin complex essential for platelet aggregation, *Science 301*, 222−226.
20. Stultz, C. M., White, J. V., and Smith, T. F. (1993) Structural Analysis Based on State-space Modeling, *Protein Sci. 2*, 305−314.
21. Celikel, R., McClintock, R. A., Roberts, J. R., Mendolicchio, G. L., Ware, J., Varughese, K. I., and Ruggeri, Z. M. (2003) Modulation of α-thrombin function by distinct interactions with platelet glycoprotein Ibα, *Science 301*, 218−221.
22. Kobe, B., and Kajava, A. V. (2001) The leucine-rich repeat as a protein recognition motif, *Curr. Opin. Struct. Biol. 11*, 725−732.
23. Kajava, A. V. (1998) Structural diversity of leucine-rich repeat proteins, *J. Mol. Biol. 277*, 519−527.
24. Kobe, B., and Deisenhofer, J. (1994) The leucine-rich repeat: A versatile binding motif, *Trends Biochem. Sci. 19*, 415−421.
25. Huizinga, E. G., Tsuji, S., Romijn, R. A. P., Schiphorst, M. E., de Groot, P. G., Sixma, J. J., and Gros, P. (2002) Structures of glycoprotein Ibα and its complex with von Willlebrand factor A1 domain, *Science 297*, 1176−1179.
26. Uff, S., Clemetson, J. M., Harrison, T., Clemetson, K. J., and Emsley, J. (2002) Crystal structure of the platelet glycoprotein Ib(α) N-terminal domain reveals an unmasking mechanism of receptor activation, *J. Biol. Chem. 277*, 35657−35663.
27. Schulman, B. A., Carrano, A. C., Jeffrey, P. D., Bowen, Z., Kinnucan, E. R., Finnin, M. S., Elledge, S. J., Harper, J. W., Pagano, M., and Pavletich, N. P. (2000) Insights into SCF ubiquitin ligases from the structure of the Skp1-Skp2 complex, *Nature 408*, 381−386.
28. Howitt, J. A., Clout, N. J., and Hohenester, E. (2004) Binding site for Robo receptors revealed by dissection of the leucine-rich repeat region of Slit, *EMBO J. 23*, 4406−4412.

BI0517483